

Synthesis of Polymer-Embedded Metal, Semimetal, or Sulfide Clusters by Thermolysis of Mercaptide Molecules Dissolved in Polymers

Luigi F. Nicolais¹ and Gianfranco Carotenuto^{2,*}

¹Dipartimento di Scienza della Comunicazione, Università di Salerno, Via Ponte - Fisciano (Salerno), Italy, ²Institute of Composite and Biomedical Materials, National Research Council, Piazzale Tecchio, 80 - 80125 Napoli, Italy

Received: August 1, 2007; Accepted: August 30, 2007; Revised: September 20, 2007

Abstract: Metal and metal sulfide clusters embedded in polymeric matrices represents a novel nanostructured material class. These materials combine optical transparency to magnetism, luminescence, UV-visible absorption, thermochromism, etc. leaving to unique functional materials that can be conveniently exploited for a number of applications in different technological fields. A really effective synthesis route for these materials is represented by the thermal decomposition of mercaptide molecules dissolved in polymer. Mercaptides can be dissolved/dispersed in polymers and thermally degraded at temperatures compatible with polymer stability (100°-250°C), generating metal atoms or metal sulfide molecules that leave to very small nanoparticles by clustering. Mercaptide synthesis, blending with polymers, and thermal decomposition are quite simple and general operations, consequently this approach can be easily applied for the preparation of a variety of nanocomposite systems. In this review, we present some fundamental aspects related to the chemistry of mercaptides (synthesis), the calorimetric study of their thermolysis process, the main techniques for nanocomposite characterization, and a short description of material applications. This article also includes recent patent coverage.

Keywords: Mercaptides, thermolysis, metal cluster, nanocomposites.

1. INTRODUCTION

A number of noble-metals, semimetals, and metal sulfides can be easily generated by thermal decomposition of mercaptides. Mercaptides are sulfur-based organic compounds, formally corresponding to thiol salts. Mercaptides are also referred as thiolates and linear alkane-thiolates (i.e., $MeSC_nH_{2n}$) represent the most common mercaptide class.

Depending on the mercaptide type, and precisely on the nature of the metal-sulfur bond, the inorganic product of thermolysis can be the pure element or its binary compounds with sulfur. In particular, covalent mercaptides (e.g., mercaptides of noble metals and semimetals) leave to a pure zero-valence solid phase, while ionic mercaptides (e.g., mercaptides of IV-Period transition metals) give the metal sulfide (i.e., Me_xS_y) as thermolysis product. There are also a few examples of mercaptides whose thermolysis gives a mixture of metal and sulfide as decomposition product (e.g., antimony mercaptide, $Sb(SR)_3$ and silver mercaptide, $AgSR$). The mechanisms involved in these two thermolysis reactions are quite different (see Fig. 1). When thermolysis produces a metal or a semimetal phase, the reaction mechanism is based on the homolytic dissociation of the metal-sulfur bonds with formation of RS radicals, which combine together leaving to disulfide molecules ($RSSR$). Instead, ionic mercaptides are dissociated in ions at molten state, and consequently a nucleophilic substitution (referred as SN_2 pathway), involving the thiolate group, RS^- , and the α -carbon of another thiolate molecule, takes place during the thermal treatment giving the formation of metal sulfide and thioether

(RSR). Thiolate molecules, RS^- , are strong nucleophiles, and also the sulfur ion, S^{2-} , is a good leaving group. Examples of these two reaction schemes are the thermolysis of the following mercaptides:



Thus, the reaction mechanism is influenced by the nature of alkyl group, R^- , since mercaptides of secondary and tertiary thiols and thio-phenols cannot give nucleophilic substitution (SN_2). Thiophenol thermolysis usually gives the metal sulfide with diphenyl molecule formation as by-product. However, these ionic compounds melt and decompose at very high temperatures.

Mercaptide thermolysis takes place at quite moderate temperatures (150°-250°C). Such mild thermal conditions are absolutely compatible with thermal stability of common polymers, and consequently the thermal degradation of mercaptide molecules can be also performed with mercaptide dissolved into a polymeric medium. In this case, a finely dispersed inorganic solid phase, embedded in polymer, is generated. Materials based on clusters confined in polymeric matrices are named nanocomposites [1-4]. Both semiconductor-polymer and metal-polymer nanocomposites have unique functional properties that can be exploited for applications in several advanced technological fields (e.g., optics, non-linear optics, magneto-optics, photonics, optoelectronics, etc.) [1].

According to the described reaction schemes, in addition to the inorganic phase, the mercaptide thermal decomposition produces also disulfide or thioether molecules as organic by-product. In some cases, these molecules are strongly chemisorbed on the surface of the produced metals

*Address correspondence to this author at the Institute of Composite and Biomedical Materials (IMCB), National Research Council, Piazzale Tecchio, 80 - 80125 Napoli, Italy, Tel: (+39) 081 7758833; Fax: (+39) 081 7758834, E-mail: giancaro@unina.it

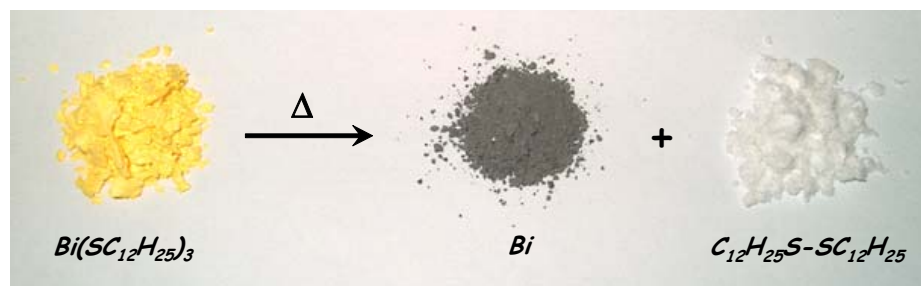
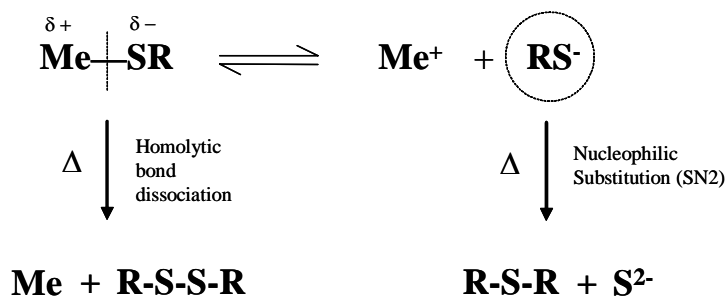
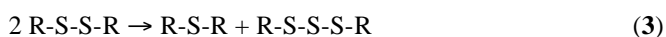


Fig. (1). Mechanistic pathways of mercaptide thermal decomposition and one example of products generated by the bismuth mercaptide thermolysis.

(e.g., gold, palladium, platinum, silver, etc.), but also in the case of a sulfide product they can be physically adsorbed, leaving to polymer-embedded cluster compounds (i.e., $\text{Me}_x(\text{SR})_y$, with $y \ll x$) at reaction end. In other cases, the RSR or RSSR molecules are dissolved in the polymer matrix, causing a light plasticizing effect (typically, a lowering in the polymer glass-transition temperature is observed). At very high temperatures (300°-400°C) the disulfide molecules convert to thioether and polysulfides, according to the following reaction scheme:

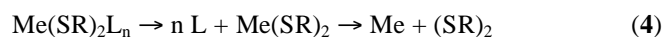


The mercaptide thermolysis reaction is well-known in organic chemistry, and it may represent a chemical route for thioether syntheses. However, the above reaction schemes have been only recently considered for the generation of inorganic solids. In particular, the use of mercaptides to produce semiconductor sulfide films on ceramic substrates has been proposed in the literature [5]. Mercaptides of gold and silver have been also used to make special inks for the metallization of pottery and ceramic substrates [6-11]. More recently, mercaptides have been used to generate finely dispersed inorganic phases inside a polymeric matrix (nanocomposites) [12-14], and a 'solvent-less' approach for the production of monodispersed nanostructures has been also proposed [15-17].

Usually, covalent mercaptides are characterized by a high solubility in non-polar organic media like ethers, hydrocarbons, chlorurate hydrocarbons, etc.; consequently these compounds may dissolve into hydrophobic polymers (e.g., polystyrene, poly(methyl methacrylate), polycarbonate, poly(vinyl acetate), etc.). Mercaptide/ polymer blends are

prepared by solution-casting technology (to prevent mercaptide decomposition before the thermal annealing treatment). Both mercaptide and polymer are dissolved into an organic solvent, then this mixture is cast on a glassy plate (e.g., Petry dish) and the solvent is slowly allowed to evaporate in air at room temperature. A slow solvent removal is required to avoid mixture cooling with mercaptide precipitation. Contact-free dispersions of particles in polymer result from the thermal annealing of homogeneous mercaptide/polymer blends. In addition, this approach gives very small (from a few nanometers to a few nanometer tens) and monodispersed clusters. The solubility of ionic mercaptides into hydrophobic polymers is quite low, but it can be improved by increasing the size of the alkyl group (-R). Usually, covalent dodecyl-mercaptides (e.g., $\text{AgSC}_{12}\text{H}_{25}$) are moderately soluble in polystyrene, while octadecyl-mercaptides (e.g., $\text{AgSC}_{18}\text{H}_{37}$) are quite soluble.

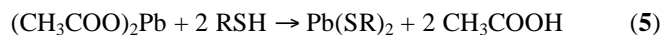
The scarce solubility of mercaptide molecules in most organic media is related to their polymeric nature. In fact, sulfur-bridges among the metal atoms are frequently present in the crystalline structure (lamellar structure) of these sulfur-based compounds. Such polymeric structures can be completely destroyed by treatment with strong ligand molecules like N-methyl-imidazole, which coordinate to the metal atoms, preventing the formation of sulfur-bridges (i.e., $[\text{Me}(\text{SR})_2]_x + nx \text{L} \rightarrow x\text{Me}(\text{SR})_2\text{L}_n$). Etheroleptic mercaptides are much more soluble than the corresponding homoleptic compounds, and their thermolysis takes place in two steps: (i) imidazole ligand lost and (ii) metal-sulfur bond cleavage at a higher temperature.



For a controlled and uniform heating of the mercaptide/polymer blends, samples are shaped in form of films which are annealed on a hot-plate at temperatures ranging from 150°C to 200°C. Both film surfaces must be simultaneously heated, and therefore they are placed between two heated metallic surfaces. Thermal gradients on the heating surface must be limited by interposing a large metallic block (heat reservoir) between sample and heat source. Thermal annealing of mercaptide/polymer blends can be also performed by using infra red lamps or a low-energy laser spot (ca. 100mW).

2. MERCAPTIDE PREPARATION

Most mercaptides are not commercially available products, since large-scale applications of these chemical compounds are quite limited (only mercaptides of tin and antimony are industrially used as thermal stabilizers for poly(vinyl chloride) [18,19]), however, these compounds can be synthesized in a very simple way. Owing to their low water solubility, mercaptides can precipitate by reacting thiols (or thio-phenols) with aqueous solutions of the corresponding metal salts. Mercaptides of mercury, lead, zinc, and copper are well-known substances and many others have been prepared (for example, mercaptides of silver, gold, platinum, palladium, iridium, nickel, iron, cobalt, antimony, bismuth, cadmium, etc.).

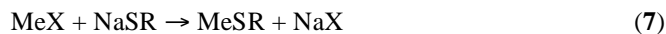


A high reaction yield characterizes the synthesis of most mercaptides and it is related to the non-polar mercaptides nature. Some mercaptides have a so low solubility in water and alcohols that promptly precipitate from these media also in the case a strong acid is simultaneously generated (for example, when thiols are reacted with silver nitrate). However, to achieve complete mercaptide precipitation, the acid by-product should be neutralized, or the reaction should be performed using metal salts of weak-acids (like mercury cyanide, mercury oxide, lead acetate, etc.).

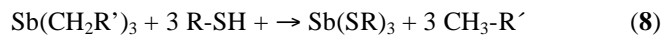
Owing to the reductant nature of thiols, a change in the oxidation number of metallic ions can be observed before mercaptide precipitation (e.g., Au(III) ions are reduced to Au(I) before mercaptide precipitation). In addition, in the case of polyvalent metals, intermediate reaction products can be obtained, since the mercaptide formation takes place by steps. For examples, chlorides of alkylmercapto-mercury can be obtained from the reaction of thiols with mercury chloride.



Mercaptides should be stored into a dry environment (desiccator cabinet) to avoid hydrolysis with thiol and metal hydroxide formation. In addition, some mercaptides can be oxidized in air, for example lead mercaptides of high-molecular weight thiols are soluble in hydrocarbons but leave to insoluble peroxides by reaction with atmospheric oxygen. Mercaptide of heavy metals give exchange reaction and in some cases it may represent a useful synthetic route.



Since thiols are acid compounds (hydrosulfuric acid derivatives), mercaptides can be also obtained by reacting them with organometallic compounds [20,21]:



The preparation of nanocomposite materials by thermolysis of mercaptide molecules dissolved in polymer represents a quite universal approach and this reaction scheme is only limited by the ability to synthesize the mercaptide precursor. A short description of most common mercaptide preparation follows:

Bismuth mercaptide. Bismuth(III) dodecyl-mercaptide, $\text{Bi}(\text{SC}_{12}\text{H}_{25})_3$, was synthesized by reacting stoichiometric amounts of dodecanethiol ($\text{C}_{12}\text{H}_{25}\text{SH}$, Aldrich) and bismuth(III) chloride (BiCl_3 , Aldrich). Both reactants were dissolved in ethyl alcohol (99,8%, Fluka) at room-temperature, and these solutions were mixed together under stirring. The presence of a little amount of water in ethyl alcohol caused the formation of bismuth hydroxide ($\text{Bi}(\text{OH})_3$). Consequently, a few drops of HCl solution were added to the alcoholic bismuth salt solution in order to dissolve this hydroxide. Mercaptide precipitation did not take place just after the reactant mixing, but the addition of ammonium hydroxide ($\text{NH}_3\cdot\text{H}_2\text{O}$, Aldrich) to neutralize the equilibrium HCl was required. Bismuth dodecyl-mercaptide was a waxy solid of yellow color, characterized by a melting point of 64°C. The mercaptide was isolated by vacuum-filtration and purified by dissolution/precipitation from chloroform/ethyl alcohol. $\text{Bi}(\text{SC}_{12}\text{H}_{25})_3$ thermo-lysis took place at very low temperature (100°C) and gave pure zero-valence bismuth.

Antimony mercaptide. Antimony(III) dodecyl-mercaptide, $\text{Sb}(\text{SC}_{12}\text{H}_{25})_3$, was prepared by adding drop-by-drop an alcoholic solution of dodecanethiol ($\text{C}_{12}\text{H}_{25}\text{SH}$, Aldrich) to an antimony chloride solution (SbCl_3 , Aldrich, 99,9%) in ethanol (99,8%, Fluka) at room-temperature, under stirring. Stoichiometric amounts of reactants were used. Mercaptide precipitation did not take place just after reactant mixing, but the addition of ammonium hydroxide ($\text{NH}_3\cdot\text{H}_2\text{O}$, Aldrich) to neutralize the equilibrium HCl was required. A white crystalline powder promptly precipitated. Such mercaptide powder was separated by vacuum-filtration, and then accurately washed with ethanol. The mercaptide was purified from NH_4Cl traces by dissolution in chloroform followed by filtration and solvent evaporation. The melting point of $\text{Sb}(\text{SC}_{12}\text{H}_{25})_3$ was of 48°C and its thermolysis gave a mixture of Sb_2S_3 (stibnite) and zero-valence antimony (90:10 respectively, as evaluated by XRD).

Silver mercaptide. Silver(I) dodecyl-mercaptide, $\text{AgSC}_{12}\text{H}_{25}$, was prepared by adding drop-by-drop an acetone solution of dodecanethiol ($\text{C}_{12}\text{H}_{25}\text{SH}$, Aldrich) to a silver nitrate solution (AgNO_3 , Aldrich, 99,9%) in acetonitrile at room temperature, under stirring [22]. Stoichiometric amounts of unpurified reactants were used. To avoid photochemical decomposition of mercaptide molecules, the reaction vessel was wrapped with an aluminum foil. A white crystalline powder promptly precipitated. The mercaptide powder was separated by pump-filtration, washed several times with acetone and stored in a dry atmosphere. The melting point of $\text{AgSC}_{12}\text{H}_{25}$ was of 180°C and it thermally

decompose at the same temperature, leaving to a mixture of zero-valence silver and silver sulfide (Ag_2S). The thermal decomposition of silver dodecyl-mercaptide in polystyrene leaves only the zero-valence silver phase [23].

Platinum mercaptide. Platinum(II) dodecyl-mercaptide, $\text{Pt}(\text{SC}_{12}\text{H}_{25})_2$, was synthesized by adding a stoichiometric amount of dodecanethiol to an alcoholic solution of Pt(IV) salt (PtCl_4 , Aldrich). Thiol reduced the platinum(IV) ions to platinum(II) before the mercaptide precipitation. Platinum(II) dodecyl-mercaptide was a crystalline orange solid. The mercaptide was separated by vacuum-filtration and accurately washed with ethyl alcohol. The thermal decomposition of $\text{Pt}(\text{SC}_{12}\text{H}_{25})_2$ gave pure zero-valence platinum.

Palladium mercaptide. Palladium(II) nitrate ($\text{Pd}(\text{NO}_3)_2$, Aldrich) and dodecanethiol ($\text{C}_{12}\text{H}_{25}\text{SH}$, Aldrich) were used to synthesize palladium(II) dodecyl-mercaptide (i.e., $\text{Pd}(\text{SC}_{12}\text{H}_{25})_2$). Both reactants were not further purified. The palladium salt was dissolved in heptane and a thiol solution in heptane was added to it under magnetic stirring. The resulting solution had a strong orange coloration and mercaptide was completely precipitated by adding some ethanol to this system. The solid precipitate was separated by vacuum-filtration and washed with acetone. Then, it was purified by dissolution/precipitation from chloroform/ethanol. The thermal decomposition of $\text{Pd}(\text{SC}_{12}\text{H}_{25})_2$ gave pure zero-valence palladium.

Gold mercaptide. Gold(I) dodecyl-mercaptide (i.e., $\text{AuSC}_{12}\text{H}_{25}$) was synthesized by treating an ethanol solution of gold tetra-chloroauric acid ($\text{HAuCl}_4 \cdot 3\text{H}_2\text{O}$, Aldrich) with an ethanol solution of 1-dodecane-thiol ($\text{C}_{12}\text{H}_{25}\text{SH}$, Aldrich), at room temperature under stirring. Au(III) was first reduced to Au(I) and then it precipitated as mercaptide ($\text{AuSC}_{12}\text{H}_{25}$). The obtained light-yellow solid phase was separated by filtration and washed with acetone. The mercaptide can be recrystallized from chloroform and its thermal decomposition at ca. 160°C gave the pure zero-valence gold.

Iron mercaptide. Iron(II) dodecyl-mercaptide, $\text{Fe}(\text{SC}_{12}\text{H}_{25})_2$, was synthesized by adding a stoichiometric amount of sodium dodecyl-mercaptide ($\text{NaSC}_{12}\text{H}_{25}$) to iron(II) chloride (FeCl_2 , Aldrich). Both reactants were dissolved in distilled water and the reaction performed at room temperature under stirring. Sodium dodecyl-mercaptide was prepared by neutralizing dodecane thiol ($\text{C}_{12}\text{H}_{25}\text{SH}$, Aldrich) with sodium hydroxide (NaOH , Aldrich) in ethanol. The obtained $\text{Fe}(\text{SC}_{12}\text{H}_{25})_2$ was a microcrystalline powder of green color, which spontaneously decomposes in a few days (disproportionation), leaving to zero-valence iron and $\text{Fe}(\text{SC}_{12}\text{H}_{25})_3$ of yellow color. Similarly, iron(III) mercaptide can be obtained starting from a Fe(III) salt. The thermal degradation of Fe(II) and Fe(III) mercaptides under nitrogen produces iron sulfide.

Cadmium mercaptide. Cadmium(II) dodecyl-mercaptide (i.e., $\text{Cd}(\text{SC}_{12}\text{H}_{25})_2$) was prepared by reacting cadmium nitrate (i.e., $\text{Cd}(\text{NO}_3)_2 \cdot 4\text{H}_2\text{O}$, Aldrich) with 1-dodecane-thiol in ethanol at room temperature under stirring. White microcrystalline $\text{Cd}(\text{SC}_{12}\text{H}_{25})_2$ promptly precipitated. This mercaptide was soluble in chloroform and decomposed at 250°C leaving to a pure CdS phase.

Zinc mercaptide. Zinc nitrate ($\text{Zn}(\text{NO}_3)_2$, Aldrich) was dissolved in ethanol and an aqueous solution of ammonium hydroxide was added drop-by-drop until the metal hydroxide was completely dissolved. Then, an alcoholic solution of 1-dodecane-thiol was added to this system at room temperature under stirring and the precipitate was isolated by vacuum filtration. Zn mercaptide (i.e., $\text{Zn}(\text{SC}_{12}\text{H}_{25})_2$) was dissolved in chloroform and blended with polystyrene, leaving to translucent films after solvent removal. The thermal annealing of zinc mercaptide/polystyrene blends, performed under nitrogen at 250°C , gave a nanoscopic ZnS phase.

Cobalt mercaptide. Cobalt acetate ($\text{Co}(\text{COOCH}_3)_2$, Aldrich 99.9%) and dodecanethiol ($\text{CH}_3(\text{CH}_2)_{11}\text{SH}$, Aldrich, 99+%) have been used for the synthesis of cobalt mercaptide. Cobalt acetate was dissolved in ethanol under stirring and a solution of dodecanethiol in ethanol was added drop-by-drop to this solution. Then the precipitate was isolated by vacuum filtration and it was washed by acetone. Cobalt mercaptide was quite soluble in non-polar organic solvents and its thermal decomposition gave a pure CoS phase.

Nickel mercaptide. Sodium dodecanethiolate ($\text{NaSC}_{12}\text{H}_{25}$) was prepared by neutralization of thiol in ethanol, using a stoichiometric amount of sodium hydroxide. The obtained sodium thiolate was isolated by ethanol evaporation using a rotovapor apparatus, and then it was dissolved in distilled water and added to an aqueous solution of nickel chloride (NiCl_2 , Aldrich). A dark-brown waxy solid of $\text{Ni}(\text{SC}_{12}\text{H}_{25})_2$ promptly precipitated and it was isolated by vacuum filtration.

Copper mercaptide. Copper acetate ($\text{Cu}(\text{OOCCH}_3)_2$, Aldrich) and dodecanethiol ($\text{CH}_3(\text{CH}_2)_{11}\text{SH}$, Aldrich) were used to synthesize copper(II) dodecyl-mercaptide. The salt was dissolved in ethanol and mixed with an alcoholic solution of thiol at room temperature, a green mercaptide precipitate was isolated by vacuum-filtration and washed by acetone. Copper(I) dodecyl-mercaptide was obtained in a similar way starting from copper(I) chloride (CuCl , Aldrich).

Many other mercaptides can be obtained using a chemical route similar to that above described. However, some mercaptides (e.g., Tl-based mercaptides) cannot be produced by such simple precipitation method because the metallic ions are promptly reduced by the thiol.

3. PRELIMINARY STUDY OF PURE MERCAPTIDE THERMOLYSIS BEHAVIOR BY THERMAL ANALYSIS

Mercaptide thermolysis may behave differently in presence or absence of polymers [24], however in most cases the inorganic phase generated by thermal degradation of mercaptide molecules dissolved in polymer corresponds exactly to that resulting from the thermal degradation of pure mercaptide. Consequently, a preliminary study of pure mercaptide thermolysis by thermal analysis approaches (DSC and TGA) is usually performed before nano-composite preparation and characterization.

Many thermodynamic information on the behavior of mercaptide thermolysis can be achieved by differential scanning calorimetry (DSC). In fact, the DSC-thermogram

of a mercaptide includes details on the number of physical and chemical transformations involved in the thermolysis (i.e., thermolysis reaction and phase transitions), nature of heats released during the transformations (exo- or endothermic process), and main thermodynamic parameters related to these processes (e.g., temperatures, reaction heats, etc.). As an example, Fig. 2 shows a typical DSC test, consisting in a dynamic run performed on bismuth mercaptide crystalline powder. DSC runs were made from room-temperature to a temperature higher than the mercaptide decomposition point, under fluxing nitrogen, and using sealed aluminum capsules to avoid changes in the thermogram baseline due to the evaporation of organic by-products. In order to identify the phases generated during the mercaptide thermolysis, DSC tests on two references (dodecylthioether, m.p. 38°C, dodecyldisulphide, m.p. 34°C, etc.) were required. The DSC thermogram of pure $\text{Bi}(\text{SC}_{12}\text{H}_{25})_3$ in Fig. 2 (performed at 10°C/min) includes three quite intensive endothermic signals and one broad exothermic signal. The endothermic signal at 64°C corresponds to the bismuth mercaptide melting point, the less intensive signal at 120°C is produced by the bismuth mercaptide thermal decomposition, and the very small peaks in the range 269-271°C are probably due to the melting of the produced zero-valence bismuth. The broad exothermic peak appearing in the range 150°-200°C is related to the clustering of bismuth atoms coming from the mercaptide molecules thermal degradation. As visible, the generated bismuth phase has a melting point lower than the characteristic value of bulk bismuth (i.e., 271°C), such a phenomenon follows to the metal melting point depression caused by the high surface free energy content of small metal clusters [14]. If a further DSC run is performed on the same sample (see Fig. 2), only two endothermic signals may be detected: the first at 38°C corresponded to the melting of the organic by-product (thioether/polysulfur mixture) which is produced by the thermal degradation of the disulphide, the second signal was that corresponding to the bismuth melting. When the thermolysis reaction involved mercaptide molecules dissolved in polymer, a similar behavior of DSC-thermogram was obtained. Similarly, the second DSC run (see Fig. 2c) included the melting of generated bismuth phase in addition to the glass-transition temperature of polystyrene (ca. 76.4°C). The absence of further melting signals and the lowering of polystyrene glass transition temperature is indicative of the organic by-product dissolution in the polymer matrix.

Thermogravimetric analysis (TGA) of pure mercaptides represents a very simple method to establish the nature of the thermolysis product. In particular, since the organic by-product of thermolysis can be completely removed by evaporation at temperatures close to 300°C (for dodecyl-derivatives), the residual weight of the inorganic solid may correspond to the percentage of metal or sulfide in the mercaptide compound. A simple comparison of the calculated metal percentage in the mercaptide with experimental residual weight allows to establish the type of thermolysis reaction (see Fig. 2d). However, such analytical approach may give useful results only by using high-purity (re-crystallized) mercaptide samples.

4. CLUSTER FORMATION IN POLYMERIC MEDIA

In the preparation of hyperfine solid systems, it is of a fundamental importance to prevent particle aggregation. Owing to the limited Brownian motions in high viscous media, particle aggregation is fully prevented if the nanoscopic solid phase is generated in polymers. Amorphous thermoplastics are characterized by elevated viscosity values also above the glass-transition temperature, and therefore they can be considered as ideal matrices for generating (nucleation/growth) nanoscopic solid phases. This medium should be preferentially selected among those polymers with a glass transition temperature (T_g) lower than the metal precursor decomposition temperature.

To increase the ability of polymers to protect particles from aggregation also a certain interaction between polymer and solid surface (polymer physical absorption) is required. Amorphous polystyrene represents a quite good material for cluster formation/growth since glass transition temperature (ca. 80°C) is closed to usual mercaptide decomposition temperatures (120-160°C) and the polymer has a certain protective ability for the presence of side-groups that may be physically absorbed on the electrophilic metal surface (π -electron density donation from phenyl groups to the metal). On the contrary, polyethylene has a low glass transition temperature value (ca. -80°C) and has not ability to protect particles from aggregation by surface absorption. It has been experimentally proved that mercaptide decomposition in polyethylene medium always leaves to a completely aggregate metallic phase.

The type of polymeric medium used for mercaptide decomposition may influence the final shape of the achieved nano-particles. In particular, the faces of a metal crystal have a different ability to bond nucleophilic species, because the acidity of absorption sites depends on the metal coordination number. The quite low ability of polystyrene side-groups to be absorbed on the crystal faces is not enough to discriminate between them. Owing to the ester functions in the poly(vinyl acetate) side-groups, these molecules are preferentially absorbed on the most acid faces of the metallic crystals. Polymer absorption creates a diffusion barrier on these crystal faces, thus inhibiting their development and simplifying the polyhedral geometry. To observe such a differential growth of the crystal faces a significant crystal development is required. For such a reason, mercaptide should be slowly decomposed to generate the metal atoms required to grow nuclei by surface deposition. For example, in the growth of triangular gold plates, the mercaptide thermal decomposition was performed at 160°C and the annealing treatment required more than 30 minutes to allow significant growth of metal crystals with a differential development of crystal faces (see Fig. 3). Finally, according to the LaMer model for monodispersed particle formation [25], a single nucleation stage must take place during the process, and then the generated nuclei should grow by addition of gold atoms to the crystal surface. During the growth stage the most acid faces do not significantly develop because of polymer absorption, leaving to a simple geometrical shape.

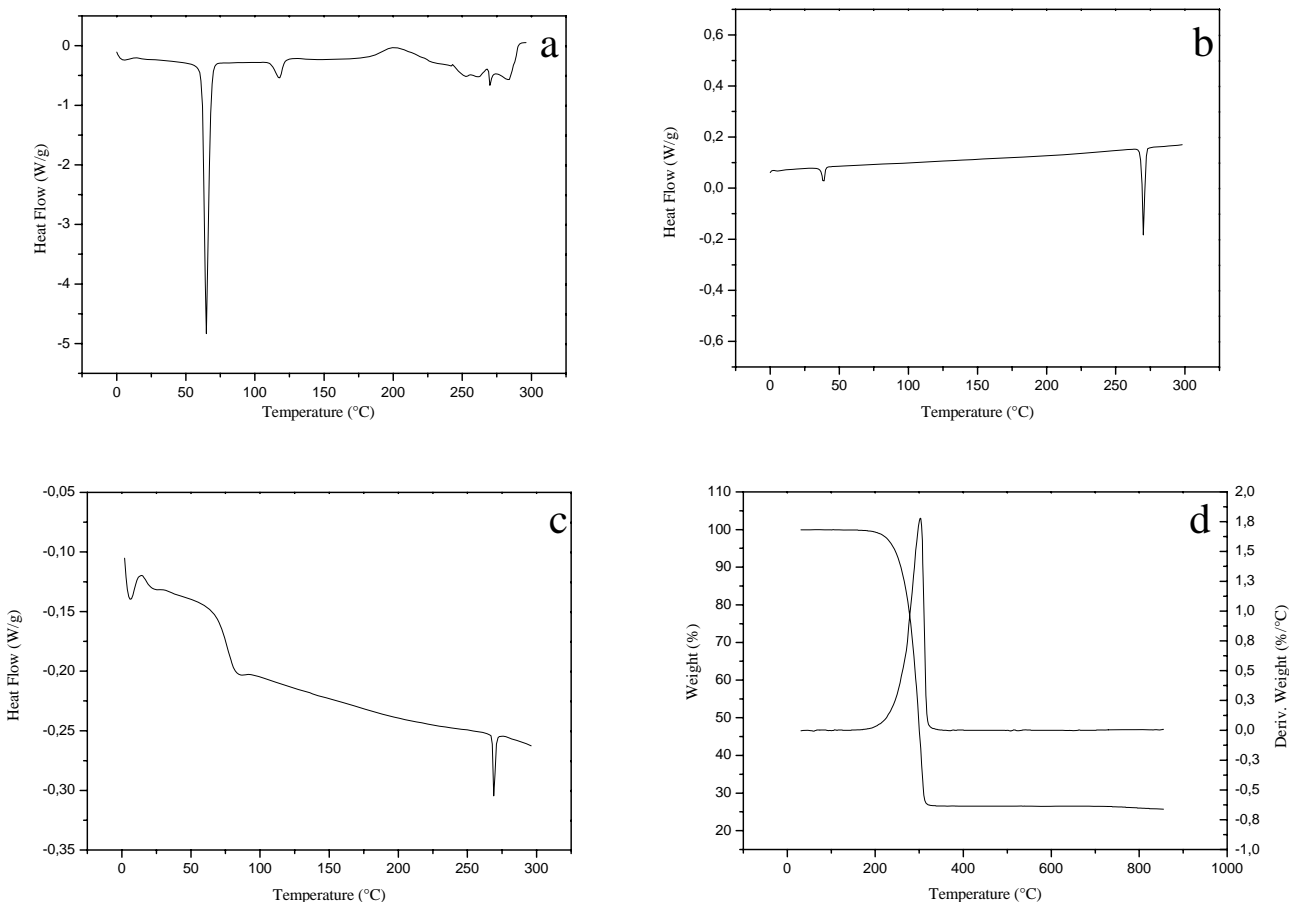


Fig. (2). Thermal analysis of the bismuth dodecyl-mercaptide: (a) DSC-thermogram (first scan) of pure $\text{Bi}(\text{SC}_{12}\text{H}_{25})_3$; (b) DSC-thermogram (second scan) of pure $\text{Bi}(\text{SC}_{12}\text{H}_{25})_3$; (c) DSC-thermogram of a thermally annealed $\text{Bi}(\text{SC}_{12}\text{H}_{25})_3$ /polystyrene blend; (d) TGA-thermogram of pure $\text{Bi}(\text{SC}_{12}\text{H}_{25})_3$.

To generate very small metal clusters (i.e., clusters with a size of only a few nanometers) a continuous nucleation regimes should be realized during the phase precipitation process. Continuous nucleation requires a high nucleation rate which can be achieved by decomposing the mercaptide at high temperature (300-400°C). Usually, in addition to the very small size the generated clusters (nuclei) show a pseudo-spherical shape and result quite monodispersed.

5. NANOCOMPOSITE MORPHOLOGY AND TOPOLOGY

Because of the very small size of generated nanoparticles (typically from a few nanometers to a few nanometer tens) and their embedded nature, the nanocomposite inner microstructure can be conveniently imaged only by Transmission Electron Microscopy (TEM) and in some cases High-Resolution Transmission Electron Microscopy (HR-TEM) is required. Owing to the significant difference in the cross-sections of atoms involved in the nano-composite guest and host phases, usually high quality TEM-micrographs are obtained (high contrasted images). TEM investigation gives information about both morphology of embedded particles (e.g., size, shape, orientation, etc.) and topology of the particle system (uniform cluster dispersion, presence and

type of aggregates, etc.). The TEM-specimen preparation is quite simple: the nanocomposite is dissolved in an adequate organic solvent under sonication, then a drop of this colloidal dispersion is placed on the TEM copper grid and solvent removed by evaporation. Such polymeric layer should be very thin (thickness inferior to 80nm) to avoid artifacts in the TEM images. Usually, a graphitization stage follows in order to reduce phase contrast and to increase the stability of sample under electron beam. However, for topological investigations, TEM-specimens must be prepared by slicing the nanocomposite piece with a cryo-ultramicrotome, since the special topology generated during the annealing treatment can be significantly modified if sample is prepared by dissolution in solvent.

(Figs. 3a,b) show the internal structure of a nanocomposite sample obtained by annealing a $\text{AgSC}_{12}\text{H}_{25}$ /polystyrene blend for 5 min at 170°C. As visible, an uniform, contact-free distribution of metal particles resulted inside these films. Particles have a pseudo-spherical shape with a size of a few nanometers, they are quite monodispersed and without aggregates. However, as shown in (Fig. 3c) for nanocomposites based on gold clusters, when the solvent was quickly evaporated during the blend preparation stage, an unusual morphology characterized by

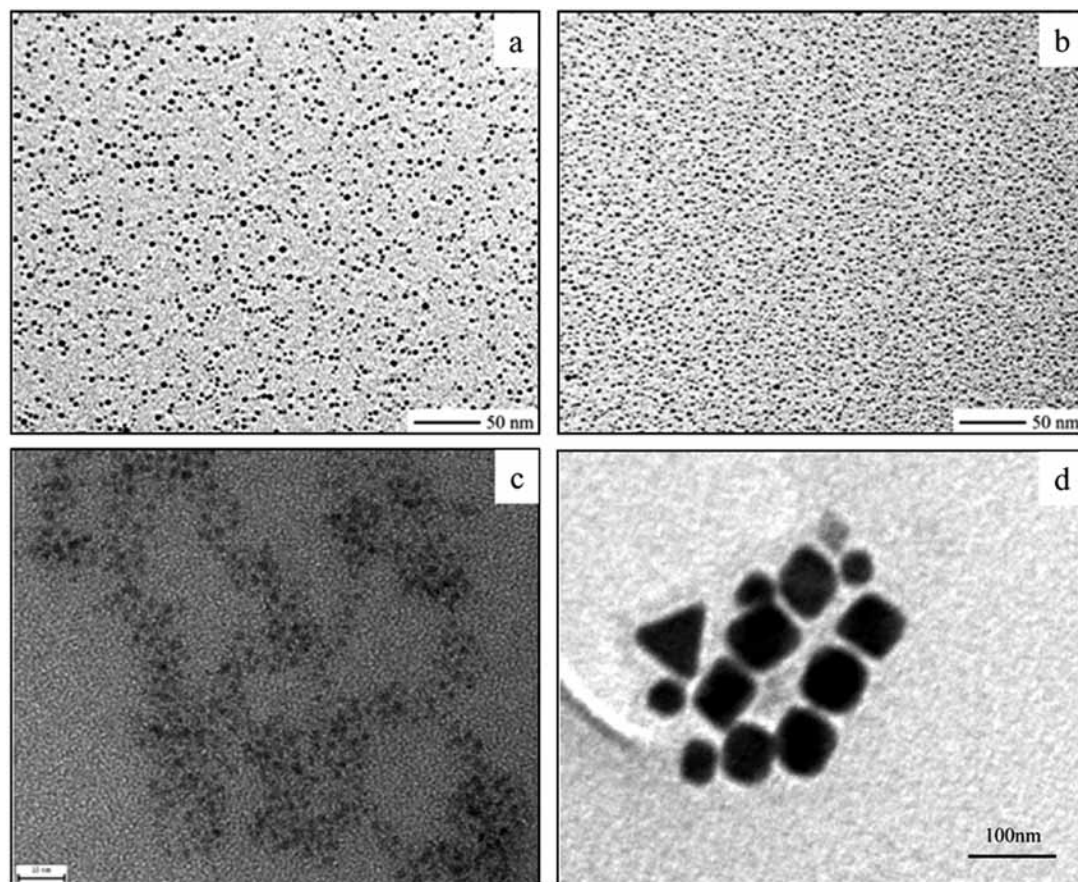


Fig. (3). TEM-micrographs showing the nanocomposite inner microstructure: (a) silver/polystyrene nanocomposite (3% by weight of $\text{AgSC}_{12}\text{H}_{25}$); (b) silver/polystyrene nanocomposite (10% by weight of $\text{AgSC}_{12}\text{H}_{25}$); (c) gold/polystyrene nanocomposite (3% by weight of $\text{AuSC}_{12}\text{H}_{25}$); and (d) gold/poly(vinylacetate) nanocomposite (thermally annealed for 30min at 160°C).

cluster aggregates embedded in polystyrene appeared. In these nanocomposite films, metal clusters were organized in two dimensional superstructures of different extension. Probably, such special organization of gold clusters was a result of local gradients in the mercaptide concentration. Aggregates were probably generated in the areas where a higher mercaptide concentration was present. Such aggregate topology was observed also in other types of nanocomposite materials. (Fig. 3d) shows gold nano-plates developed during the thermal annealing of a $\text{AuSC}_{12}\text{H}_{25}$ /poly(vinylacetate) blend for 30min. As visible, nanoparticles of regular shapes are generated in this system, probably for the ability of the acetate groups present in the embedding polymer to selectively bond the different crystallographic faces of growing gold crystals.

6. NANOCOMPOSITE STRUCTURAL CHARACTERIZATION

Usually, the inorganic phases generated by thermal decomposition of mercaptide molecules have a crystalline nature and therefore they can be simply identified by large-angle X-Ray Powder Diffraction (XRD). Owing to the small size of the crystalline domains (inferior to 50nm), the diffraction pattern of such polymer-embedded nano-crystals is made of quite broad signals. In addition, the percentage of inorganic phase in a nanocomposite sample is usually low,

and consequently peaks are of low intensity. Only those signals corresponding to the most abundant crystallographic planes can be detected and a low signal/noise ratio characterizes most nanocomposite diffractograms (see Fig. 4). Diffraction data of good quality can be achieved only by a slow angular movement of detector and using X-ray sources with adequate anti-cathode materials. Generally, nanoparticles are single crystals, consequently the broadening of the diffraction peaks allows an approximate evaluation of crystallite size by the Scherrer's formula and the distribution of peak intensities may give also an idea of nanoparticle shape.

The electronic absorption spectra (UV-visible-NIR) of polymer-embedded metal clusters contain valuable information on their electronic structure and bonding. They illustrate the way in which metallic properties develop in clusters of large enough size. Unfortunately, there has been little systematic study of the electronic spectra of metal cluster compounds, although this approach can give important structural information. A short description of characterization by UV-Vis spectroscopy of clusters of different nuclearity follows.

Low-nuclearity clusters (i.e., molecular clusters) embedded in polymer show relatively simple electronic absorption spectra which are typical of molecules with well-spaced

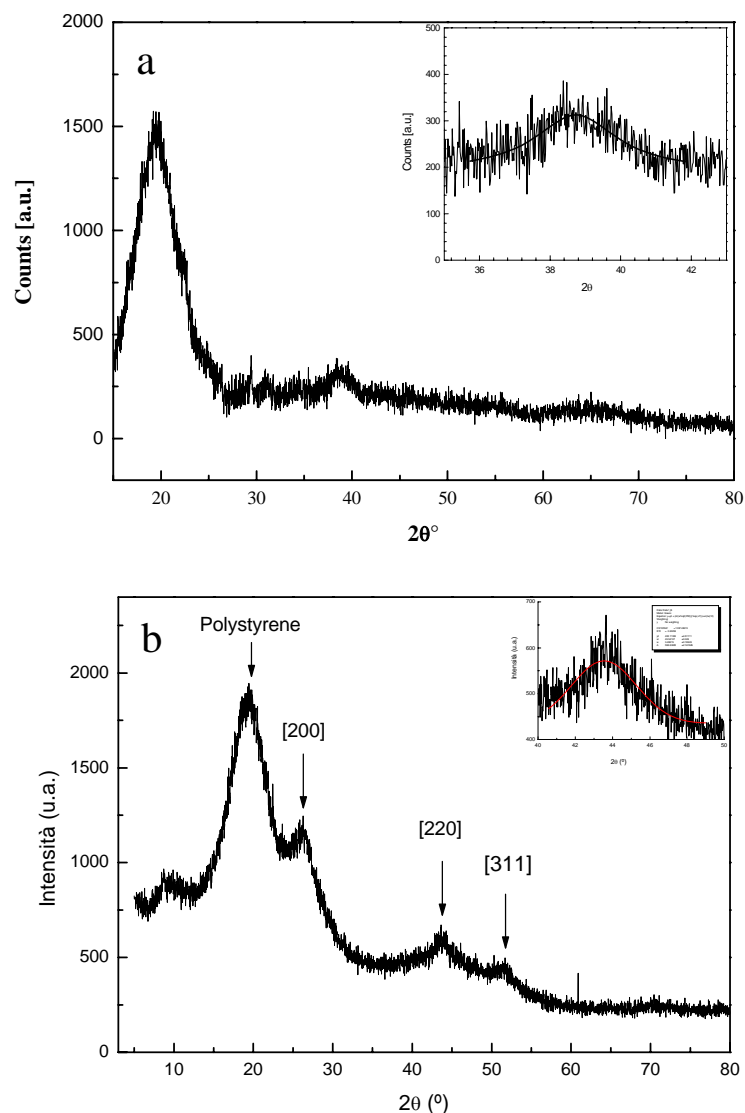


Fig. (4). Large angle X-ray powder diffraction (XRD) of: (a) gold/polystyrene nanocomposites; (b) CdS/polystyrene nanocomposites.

electronic energy levels. Absorptions of polymer side-groups occur in the ultra-violet region, and they can be compared with the absorptions of free groups, to study the effect of coordination to metal cluster surface. Metal cluster absorptions occur mainly in the UV and visible regions, extending in some cases into the near infra-red. In principle, each absorption can be assigned (as $\sigma \rightarrow \sigma^*$, etc.) with the longest wavelength absorption corresponding to the HOMO-LUMO gap if this transition is symmetry-allowed. In practice, it can be achieved only for spectra of relatively small clusters. As the clusters get larger, the frontier orbital separation becomes smaller, and the absorption bands move across the visible region towards the near infrared. The quantitative intensities of the longest wavelength absorptions of clusters with nuclearity close to 10 are already very low. Frequently, in addition to one-electron absorption bands in the UV-visible spectra assigned to transitions between metal-metal bonding and antibonding orbitals there are bands corresponding to transitions between metal-metal bonding orbitals and ligand antibonding orbitals. On cooling, one-

electron absorption bands sharpen, because of the effect of the population of vibrational energy levels. λ_{\max} may also change, according to the Frank-Condon principle, if the metal-metal distances are not the same in the ground and excited states.

In larger clusters, the resolution of one-electron bands is lost, and a broad, continuous electronic absorption evolves, spanning the visible region into the near-infrared. This absorption reflects the overall density of states of the electronic energy levels in the cluster, with the HOMO now being equivalent to the Fermi energy. In gold clusters, it is a $5d \rightarrow 6s, 6p$ transition. At the low-energy end of the spectrum, we can now use the onset wavelength λ_{onset} to estimate the 'band gap' energy difference between the HOMO and LUMO in the cluster. This is an usual practice in the study of small clusters of semiconductors such as CdS, but it has been rarely applied to the electronic spectra of metal clusters. This highlights an unsolved problem in understanding the quantitative density of states at the Fermi level in clusters and colloids, because in colloidal gold the $5d \rightarrow 6s, 6p$

interband transition has comparable intensity only to 1050nm. At the high-energy end of the spectrum, the shape of the interband absorption in clusters is often obscured by UV absorptions within the polymer side-groups. Changing the temperature has little effect on absorption bands of this type. There may be some change in λ_{onset} as the thermal population of levels around the Fermi energy alters.

Delocalised, mobile conduction electrons within a metal particle have a characteristic collective oscillation frequency. This surface plasmon resonance is seen as an absorption band in the UV-visible spectrum of polymer-embedded clusters. Metals with s-band electronic structures show well-defined plasmon resonances in the visible region; for silver and gold, these occur respectively at wavelengths of 390nm and 520nm. These absorptions weaken as the particle size is reduced, but they can be observed for silver and gold colloids of diameter as small as 10-20Å. The weak absorption at 510nm in the Au_{55} spectrum can be a surface plasmon resonance. This 55-atom cuboctahedral gold cluster has an overall diameter (from vertex to opposite vertex) of about 14Å. The mean first-nearest-neighbor coordination number of the metal atoms, N_1 , which is a parameter correlating well with measures of metallic behavior, is 7.85. A similar suggestion had been made for $Ag_{20}Au_{18}$, which shows a strong absorption at 495nm, the same wavelength as the plasmon absorption in bimetallic $AgAu$ colloids of similar composition. However, the assignment of this band as a plasmon resonance seems unlikely since it is strange that a surface plasmon absorption could be so strong in $Ag_{20}Au_{18}$ but so weak in Au_{55} . The $Ag_{20}Au_{18}$ cluster contains fewer metal atoms than the Au_{55} one, and it is not a close-packed cluster, having a structure based on three 13-atom icosahedra aggregated into an oblate spheroid; its N_1 value is 7.18. Moreover, the effect of particle shape on the plasmon resonance frequency had not been taken into account in comparing the $Ag_{20}Au_{18}$ molecular cluster with bimetallic colloids. In an oblate cluster, any plasmon resonance absorption should occur at a wavelength significantly longer than that in a spherical particle of the same composition, and another effect of the departure from spherical symmetry is to split the resonance into two non-degenerate absorption bands. However, the 510 nm absorption in Au_{55} probably arises from aggregates of cluster molecules in solution, and that any plasmon absorption in individual Au_{55} molecules is too weak to be observed above the interband absorption. Au_{55} behaves in an almost identical manner. This limits the number and delocalization of the 6s electrons in the Au_{55} clusters. The possible reason for the absence of a clear plasmon absorption in Au_{55} is that the plasmon is broadened and dampened by interaction with the interband absorption, which acts as a decay channel. A further explanation is that the quantitative intensity, C_{abs} , of a plasmon absorption depends on the third power of the particle diameter, a, according to:

$$C_{\text{abs}} = (8\pi^2 a^3 / \lambda) \text{Im}((\epsilon - 1) / (\epsilon + 2)) \quad (9)$$

where λ is the wavelength in the medium, and ϵ is the complex relative permittivity of the metal relative to that of the surrounding medium. Even if cluster electrons are fully delocalized and able to undergo a dipole resonance, the plasmon absorption in Au_{55} might simply be too weak to

detect above the background interband absorption, which is quite intense at 520nm. So there may be no need to invoke any special broadening or damping mechanisms. In metals having a less free-electron behavior than silver and gold, absorption maxima in the UV-vis-NIR spectrum cannot be assigned as pure plasmon resonances, because they also have considerable interband character. In palladium clusters, the UV-visible band corresponds most closely to a surface plasmon absorption occurring in the UV at about 230nm. However, the optical spectrum of Pd_{561} (cluster diameter $\approx 30\text{\AA}$, with $N_1=10.05$, assuming an ideal 561-atom cuboctahedral structure) is uninformative, because this spectral region is obscured by electronic transitions within the polymer. A plasmon absorption is not usually detected from platinum clusters, but the theoretical position of this absorption band should be at ca. 240 nm. The position and intensity of a surface plasmon absorption band is unlikely to depend on temperature. This gives the possibility of distinguishing experimentally between this type of absorption and one-electron absorptions in the same region of the spectrum.

This outline of polymer-embedded cluster characterization is far from being complete. Advances in Nuclear Magnetic Resonance (NMR), SQUID-Magnetometry, and many other characterization techniques are of considerable importance as well. In fact, the technological success of a nanostructured material strictly depends on the study of physical properties.

7. NANOCOMPOSITE APPLICATIONS

Metal-polymer nanocomposites can be exploited for a number of technological applications. The functional uses of these materials are mainly related to their unique combination of high transparency in the visible spectral range with other physical properties (e.g., luminescence, magnetism, surface plasmon resonance, ultra high/ low refractive index, optical non-linearity, etc.). Fig. 5 shows some examples of optical devices based on metal-polymer nanocomposites.

Perfectly transparent, light-fast, color filters and UV-absorbers can be obtained by combining metal clusters of coin metals (silver, gold, etc.) with optical polymers (i.e., amorphous polymers with visible refractive index close to 1.5, like polystyrene, poly(methyl methacrylate), polycarbonate, etc.). The high extinction coefficients that characterize the surface plasmon absorption of these metals allows intensive coloration at very low filling factors, and the nanoscopic filler size make possible the realization of ultrathin color filters [26,27].

A system of aggregated particles characterized by surface plasmon resonance absorbs differently from a system of isolated particles. For example, aggregated silver clusters are characterized by a brown coloration, while isolated silver particles (contact free dispersion of silver clusters) look yellow. Consequently, a change in the inter-particle distance produced for example by an expansion of the embedding matrix may cause color switching. Nanocomposites based on polymer-embedded silver clusters containing a small amount of the mercaptide precursor shows a color change from brown to yellow at a temperature close to the mercaptide melting point [28,29]. This thermochromic phenomenon is

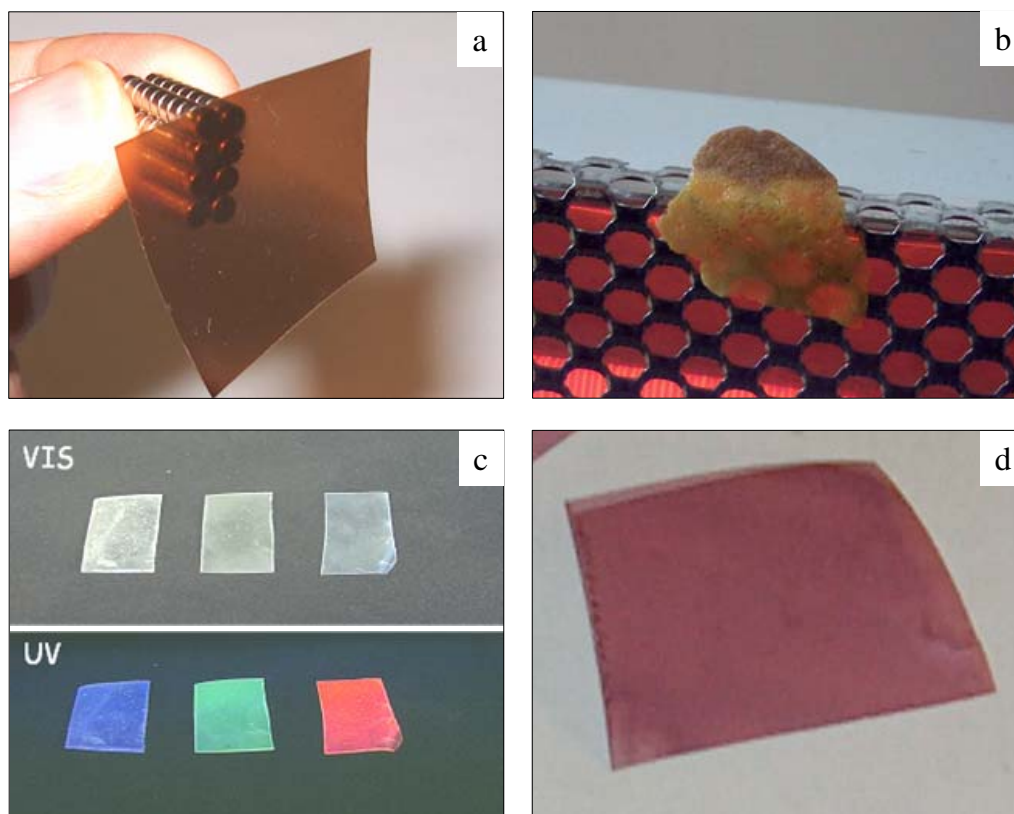


Fig. (5). Examples of applications of metal-polymer and sulfide/polymer nanocomposites: (a) ferromagnetic-transparent FeS/polystyrene nanocomposite; (b) thermochromic silver/polystyrene nanocomposite; (c) luminescent nanocomposites (ZnS/polystyrene, CdS/polystyrene, and Au/polystyrene, from left-side to right-side); and (d) color filter based on the surface plasmon resonance of gold clusters (gold/polystyrene nanocomposites).

probably related to a matrix expansion caused by the melting of thiolate molecules chemisorbed on the silver cluster surface.

Magnetic solid phases with nanoscopic dimensions do not scatter visible light, consequently their embedding into optical plastics leave to magnetic-optical materials. Magnetic particles may behave super-paramagnetically or ferromagnetically, depending on their size. In particular, when size is larger than the single magnetic domain, nanoparticles result ferromagnetic otherwise they are superparamagnetic. As a consequence, superparamagnetic and ferromagnetic optical plastics can be produced [30,31]. If particles with acicular shape are embedded in polymer, the magnetic properties can be significantly enhanced by a shape anisotropy effect. These materials can be exploited for a number of technological applications based on their transparency and/or low density (magneto-optics, magnetic levitation, optically transparent data storage systems, etc.).

Luminescent plastics are useful for a number of technological applications (e.g., photoelectric sensing, anticounterfeiting, materials for chip-on-board technology, optical filters for converting high-energy solar light to useful radiation for photovoltaic cells, advanced materials for greenhouse windows (agriculture), etc.) [32]. Plastics can be made luminescent simply by embedding of small metal and semiconductor clusters (e.g., sulfides). Such luminescence type is very attractive mainly for the possibility to control the

bandgap through material composition and size. Nanoparticles are characterized by a size and composition dependent bandgap which can be tuned atom by atom during the synthesis stage to emit at any visible or infrared wavelength. Polymer embedded nanoclusters are ready to be used with the great advantage of a very versatile manufacturing of polymers.

Further applications of metal-polymer nanocomposites are in the fields of ultra high/low refractive index materials [33-35], dichroic color filters [36,37], non-linear optical filters [38], catalytic polymer membranes [39,40], etc.

8. CURRENT & FUTURE DEVELOPMENTS

The thermolysis of mercaptide molecules dissolved in polymers represents a very simple, effective, and universal *in situ* approach for polymeric nanocomposite synthesis. In fact, clusters of different noble-metals, semimetals, and metal sulfides can be easily generated by this method in combination with all types of thermo-plastics. In addition, both contact-free cluster dispersions or aggregated topologies, with controlled cluster size and numerical density, can be obtained by this method. Such advanced material class combine versatile processing, lightness, optical transparency, etc. to magnetism, luminescence, UV-visible absorption, thermochromism, etc. leaving to unique functional materials that can be conveniently exploited for a number of applications in different technological fields (e.g., optics,

magneto-optics, non-linear optics, photonics, optoelectronics, etc.).

So far the study of this chemical route has been limited to mercaptides simply deriving from linear alkyl-thiols (i.e., $C_nH_{2n+1}-SH$), since these chemical compounds are widely spread on the market. However, future developments in this research area will involve the use complex mercaptide molecules including branched-aliphatic and aromatic groups, perfluorurate mercaptides (i.e., $C_nF_{2n+1}-SH$), mercaptides with additional functional groups at end, etc. The use of these complex mercaptide may allow complete control over the thermal decomposition process and high solubility in polar and non-polar polymers. Also the use of heteroleptic mercaptides, whose solubility in polymers is much higher than for the homoleptic counterpart will spread in the future since nanocomposites with higher filling factors can be prepared. Quite important is the availability of adequate techniques for the structural characterization of these systems, and multinuclear-NMR and Raman spectroscopies are assuming a growing importance in the study of clusters confined in polymeric matrices. Also, the possibility to use these systems as precursors in the preparation of other nanostructured materials (e.g., organic/inorganic nanotubes) by pyrolysis represents a new research area involving metal-polymer nanocomposites that will growth very quickly in the near future.

REFERENCES

- [1] Caseri W. *Macromol Rapid Commun* 2000; 21: 705-722.
- [2] Mayer ABR. *Mater Sci Eng* 1998; 6: 155-166.
- [3] Carotenuto, G., Nicolais, L.: EP1489133A1 (2004).
- [4] Carotenuto, G.: US20060121262A1 (2006).
- [5] Hasegawa, Y., Okano, K., Isozaki, Y., Tabata, M., Hayashi, C., Nakanishi, A.: US925110622 (1992).
- [6] Davlin, A.: US20016231925 (2001).
- [7] Howard, M.F.: US2994614 (1961).
- [8] Fritsche, K.-D., Dorbath, B., Giesecke, N., Ruhnau, K.: US5707436 (1998).
- [9] Howard M.F.: US2984575 (1961).
- [10] Kermit, H., Ballard, P.A.: US2490399 (1949).
- [11] Nguyen, P.H.: US894808274 (1989).
- [12] Carotenuto G, Nicolais L. *J Mater Chem* 2003; 13: 1038-1041.
- [13] Carotenuto G, Nicolais L, Perlo P. *Polym Eng Sci* 2006; 46(8): 1016-1020.
- [14] Carotenuto G, Nicolais L. 'Nanocomposites, Metal-Filled', in *Encyclopedia of Polymer Science and Technology*, 3rd Edition, John Wiley & Sons., Inc. Hoboken, NJ, USA, 2003.
- [15] Larsen TH, Sigman M, Ghezelbash A, Doty RC, Korgel BA. *J Am Chem Soc* 2003; 125: 5638-5639.
- [16] Sigman MB, Ghezelbash A, Hanrath T, Saunders AE, Lee F, Korgel B, *J Am Chem Soc* 2003; 125: 16050-16057.
- [17] Ghezelbash A, Sigman MB, Korgel BA. *Nano Lett* 2004; 4(4): 537-542.
- [18] de Sousa APG, Silva RM, Cesar A, Wardell JL, Huffman JC, Abras A. *J Organomet Chem* 2000; 605: 82-88.
- [19] Qu L, Tian W, Shu W, *Polym Degrad Stab* 2002; 76: 185-189.
- [20] Anderson KM, Baylies CJ, Jahan AHM, Norman NC, Orpen AG, Starbuck J. *Dalton Trans* 2003; 3270-3277.
- [21] Clegg W, Elsegood MRJ, Farrugia LJ, Lawlor FJ, Norman NC, Scott AJ. *J Chem Soc Dalton Trans* 1995; 2129-2135.
- [22] LaMer VK, Dinegar RH, *J Am Chem Soc* 1950; 72(11): 4847-4854.
- [23] Carotenuto G, LaPeruta G, Nicolais L. *Sens Actuators B* 2006; 114: 1092-1095.
- [24] Conte P, Carotenuto G, Piccolo A, Perlo P, Nicolais L. *J Mater Chem* 2007; 17: 201-205.
- [25] Dance IG, Fisher KJ, Herath Banda RM, Scudder ML. *Inorg Chem* 1991; 30: 183-187.
- [26] Zheng M, Gu M, Jin Y, Jin Y. *Mater Res Bull* 2001; 36: 853-859.
- [27] Carotenuto G. *Appl Organomet Chem* 2001; 15: 344-351.
- [28] Carotenuto G, LaPeruta G, Nicolais L. *Sens Actuators B* 2006; 114: 1092-1095.
- [29] Carotenuto, G., Martorana, B., Pullini, D., Perlo P., Carotenuto, G., Nicolais, L.: EP1621574 (2004).
- [30] Carotenuto G, Pepe G, Davino D, Martorana B, Perlo P, Acierio D, Nicolais L. *Micro Opt Technol Lett* 2006; 48(12): 2505-2508.
- [31] Gonsalves KE, Carlson G, Benaissa M, Jose-Yacaman M, Kim DY, Kumar J. *J Mater Chem* 1997; 7(5): 703-704.
- [32] Carotenuto G, Longo A, Repetto P, Perlo P, Ambrosio L, *Sens Actuators B Chem* 2007; 125: 202-206.
- [33] Weibel M, Caseri W, Suter UW, Kiess H, Wehrli E. *Polym Adv Tech* 1991; 2: 75-80.
- [34] Zimmerman L, Weibel LW, Caseri W, Suter UW, Walther P. *Polym Adv Tech* 1992; 4: 1-7.
- [35] Zimmerman L, Weibel LW, Caseri W, Suter UW. *Suter, J Mater Res* 1993; 8: 1742-1748.
- [36] Dirix Y, Bastiaansen C, Caseri W, Smith P. *J Mater Sci* 1999; 34: 3859-3866.
- [37] Dirix Y, Bastiaansen C, Caseri W, Smith P. *Adv Mater* 1999; 11: 223-227.
- [38] Qu S, Song Y, Liu H, Wang Y, Gao Y, Liu S, Zhang X, Li Y, Zhu Y. *Optics Comm* 2002; 203: 283-288.
- [39] Troger L, Hunnefeld H, Nunes S, Oehring M, Fritsch D. *Z. Phys D* 1997; 40: 81-83.
- [40] Fritsch D, Peinemann KV. *Catal Today* 1995; 25: 277-283.